Semicontinuous Distillation for Ethyl Lactate Production

Thomas A. Adams II and Warren D. Seider
Dept. of Chemical and Biomolecular Engineering, University of Pennsylvania, 311A Towne Building, Philadelphia, PA 19104

DOI 10.1002/aic.11585
Published online July 24, 2008 in Wiley InterScience (www.interscience.wiley.com).

A novel semicontinuous process for the production of ethyl lactate from ethanol and lactic acid is studied. The process utilizes a middle vessel integrated with a distillation column to perform a ternary separation of the reaction mixture. A pervaporation unit separates ethanol from water. This new form of process intensification is shown to be economically superior to traditional batch and continuous alternatives for a wide range of production rates. © 2008 American Institute of Chemical Engineers *AIChE J,* 54: 2539–2552, 2008

Keywords: semicontinuous, distillation, ethyl lactate, process intensification, middle vessel

Introduction

Demand for fine and specialty chemicals has been growing in recent years.[1–3] These are often produced at intermediate capacities that are above the rates typically achieved by batch systems, but not high enough to take full advantage of the economy-of-scale benefits of continuous systems. Therefore, semicontinuous processes have recently been developed to perform cost-effective separations at intermediate capacities. Semicontinuous processes are based on a forced-cyclic technique using a separation unit such as a distillation or extraction column tightly integrated with one or more middle vessels (MV). The single separation unit typically achieves the functionality of two or more units. For example, a ternary semicontinuous distillation (SD) process separates a three-species mixture with only one distillation column and one tank used as a middle vessel.[4–7] Semicontinuous extractive distillation[8] and semicontinuous, azeotropic, pressure-swing distillation[9] processes have also been studied using similar single-column configurations.

The integration of reaction with SD has recently been introduced by Adams and Seider[10] for an exothermic reversible reaction in the form of $A + B \leftrightarrow C + D$. This process, called semicontinuous distillation with chemical reaction in a middle vessel (SDRMV), uses a continuous stirred-tank reactor (CSTR) as one of two middle vessels. Rigorous simulations demonstrate that the SDRMV system is a feasible method of creating and isolating the specialty chemical D, and that flooding and weeping are prevented in the single trayed-distillation column. Further economic analyses when compared with traditional batch and continuous equivalents suggest that the SDRMV process is economically preferable for a wide range of intermediate production rates.

Ethyl lactate has good solvent properties that makes it useful in a wide variety of industrial cleaning and dissolving applications.[11] It also has a low toxicity and a low health risk to humans.[12] Several methods of production have been explored, such as batch distillation with a reactive still,[13] reaction with integrated pervaporation,[14] and reaction with vapor permeation.[15] A conceptual, continuous, reactive-distillation (RD) process has been proposed[16] and recently verified experimentally.[17] In this article, a novel SD process is proposed and simulated for the production of ethyl lactate and recovery from its reaction mixture. To the best of our knowledge, the economics and operational feasibility of a ternary SD system with the proposed configuration has not yet been studied.

Additional Supporting Information may be found in the online version of this article.

Correspondence concerning this article should be addressed to W.D. Seider at seider@seas.upenn.edu.

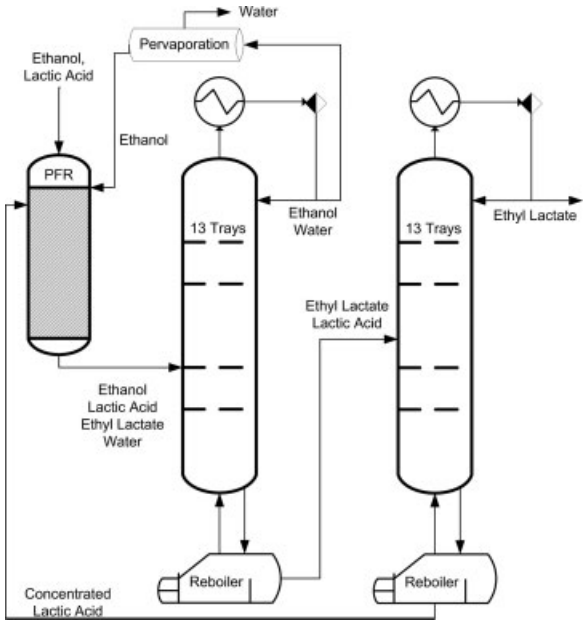

Figure 1. Continuous process.

Case Studies

Process goal

Ethanol (E) and lactic acid (LA) are reacted reversibly to form water (W) and ethyl lactate (EL), as shown below, with normal boiling points annotated:

$$\text{Ethanol } (78.3^{\circ}\text{C}) + \text{Lactic Acid } (216^{\circ}\text{C}) \leftrightarrow \text{Water } (100^{\circ}\text{C}) + \text{Ethyl Lactate } (156^{\circ}\text{C}) \quad \text{(R1)}$$

The ethyl lactate and water must be recovered individually from the reaction mixture with 98 mol % purity. The following three methods are examined: a traditional continuous process with a reactor, two distillation columns, and a pervaporation unit; a traditional batch process with a reactor, one distillation column, and a pervaporation unit; and a novel semicontinuous process with a reactor, one distillation column, and a pervaporation unit.

Continuous process

The continuous process of this study employs a plug-flow reactor (PFR), two sieve-tray distillation columns of 13 trays each, and a pervaporation unit, as shown in Figure 1. Equimolar amounts of ethanol and lactic acid are fed to the PFR. The reactor effluent, in chemical equilibrium at about 63% conversion, is fed to the first distillation column. The distillate, containing ethanol and water, is fed to a pervaporation unit, where water is removed in the permeate. The ethanol-rich retentate is recycled to the PFR, with the bottoms product, containing ethyl lactate and lactic acid, fed to the second distillation column. In this unit, ethyl lactate is recovered in the distillate, and concentrated lactic acid, recovered in the bottoms, is recycled to the PFR.

The distillation columns were modeled using the RadFrac block of Aspen Plus 2004.1 over a range of capacities varying from 10 to 225 mol/min of ethyl lactate recovered. The reflux and boilup ratios of the distillation columns were adjusted to minimize the total reboiler duty, with the requirement that only trace amounts of ethyl lactate are in the distillate of the first column, and that the ethyl lactate in the distillate of the second column is 98 mol % pure. The physical properties, chemical reaction, and pervaporation units were modeled as described in the Model Development section. The sizes of the process units scale with the production rate.

Batch process

The batch process, shown in Figure 2, operates in a seven-mode cycle, shown in Figure 3. During Mode 1, the contents of the CSTR, which contain the reaction product at chemical equilibrium, are transferred to the pot under the distillation column. The pot heating begins using steam in the jacket and coils. At high production rates, the heating is instead provided by drawing some of the liquid from the pot, heating with an external heat exchanger, and returning it to the pot. In Mode 2, the CSTR is charged with fresh ethanol and lactic acid, and concentrated lactic acid is transferred from Tank 1. Ethanol and water begin to appear together in the distillate near the azeotropic composition. A proportional-integral (PI) controller regulates the reflux ratio to ensure that the ethyl lactate in the distillate remains below 0.1 mol %. The distillate is sent to a small holdup tank (Tank 2). Throughout Modes 2–6, the contents of Tank 2 (ethanol and water) are slowly fed to a pervaporation unit, which removes the water. The ethanol-rich retentate is recycled to the CSTR. This slow-feed mechanism permits separation with a small membrane area. Consequently, for batch Case 2 (see Table 7), the slow-feed mechanism requires only 8 m^2 of membrane area at a cost of \$2591. Without the use of Tank 2, the pervaporation unit must be at least 600 m^2 to adequately separate the distillate during Mode 2 since feed

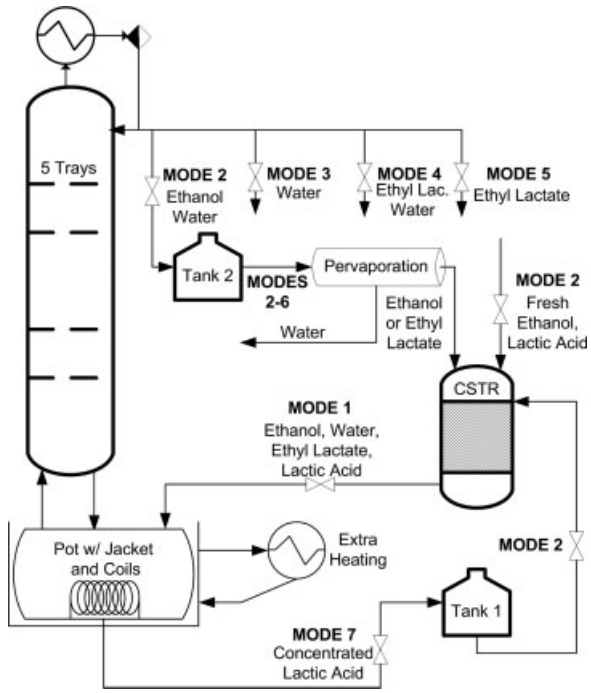

Figure 2. Batch process.

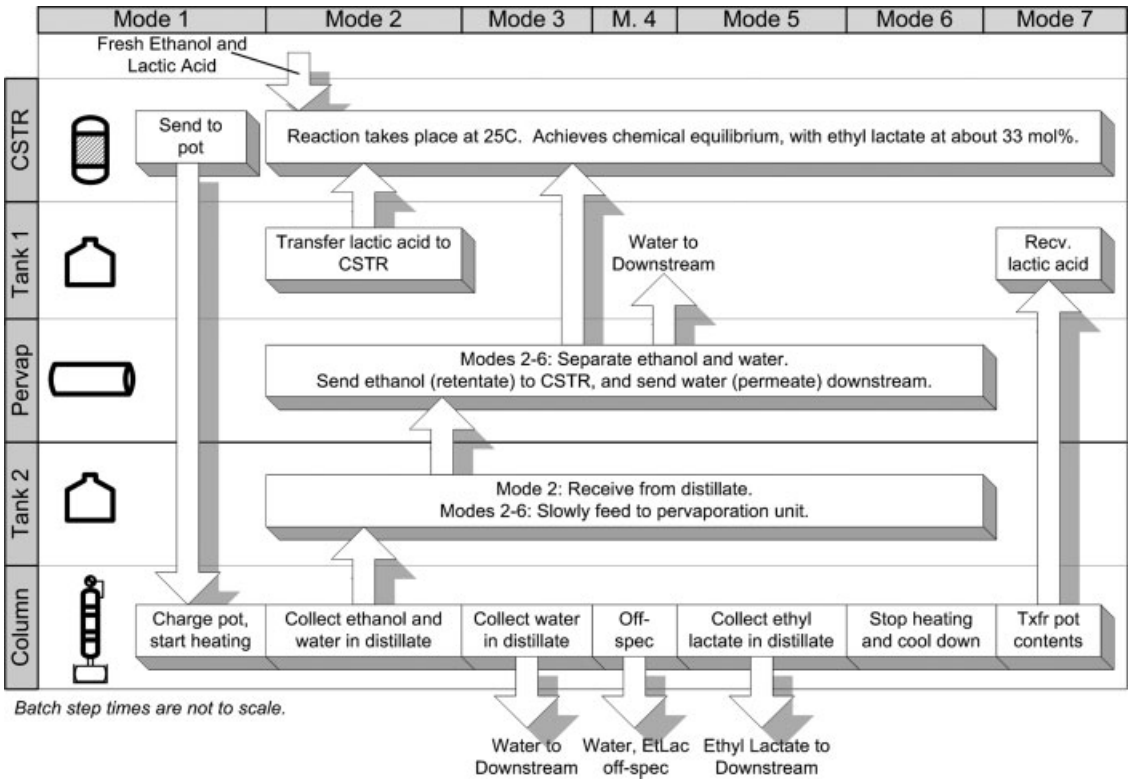

Figure 3. Schedule of the batch process units.

rates to the unit are significantly higher. The total direct cost of the 600 m^2 unit is increased greatly to \$194,350.

Mode 3 begins when the ethanol has been completely removed from the pot, leaving nearly pure water in the distillate, which is sent downstream. Once the concentration of water in the distillate falls below 95 mol %, Mode 4 begins. During Mode 4, the setpoint of the reflux ratio controller is changed to achieve 98 mol % of ethyl lactate in the distillate. During this transition, the off-specification distillate is sent downstream for further processing or recycling. Once the distillate reaches specification, Mode 5 begins, and 98 mol % of ethyl lactate is recovered in the distillate. When the ethyl lactate remaining in the pot diminishes to 3 mol %, the heating is stopped and Mode 6 begins. The liquid on the trays falls back into the pot, containing concentrated lactic acid, which is transferred to Tank 1 during Mode 7.

The simulation of the pot and distillation column was performed with Aspen BatchSep 2004.1. The physical properties, chemical reaction, and pervaporation unit were modeled as described in the Model Development section. The batch size and heat flux were varied to minimize the total annualized cost at various overall production rates. On the basis of previous cooling simulations,[10] the cool-down step of Mode 6 was assumed to last 2 h. Mode 7 was assumed to require 10 min.

Semicontinuous process

The SD process, shown in Figure 4, uses one 13-tray distillation column interacting with a middle vessel, a CSTR, and a pervaporation unit. Similar to other ternary SD processes,[4] the cycle operates with three main phases of opera-

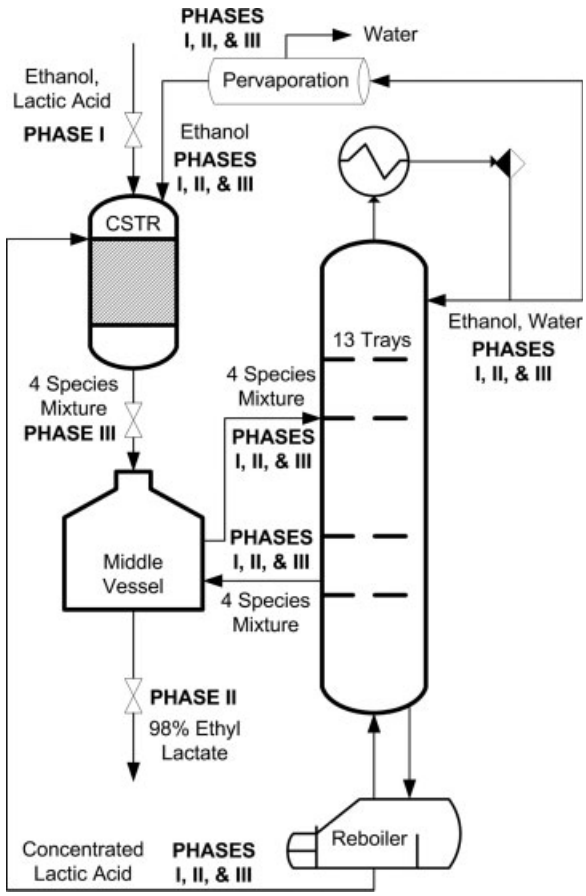

Figure 4. Semicontinuous process.

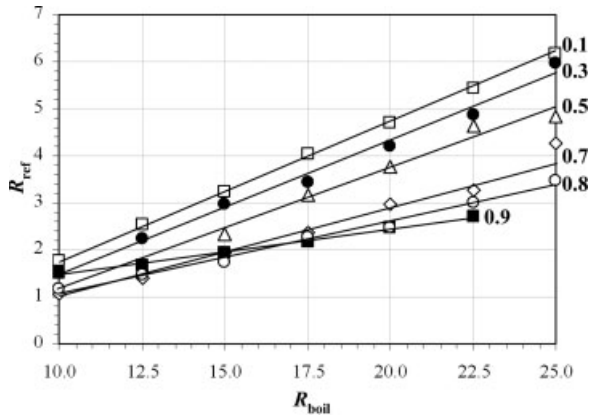

Figure 5. Optimum reflux ratios at various boilup ratios and feed compositions.

$x_{F,EL}$ is the parameter.

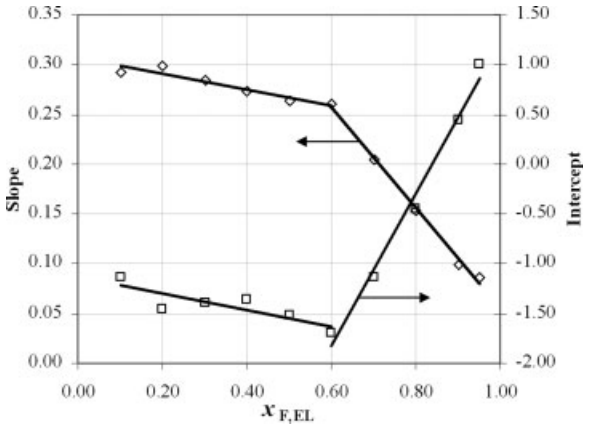

Figure 6. Slope and intercepts of the reflux- and boilup-ratio curves in Figure 5 as a function of $x_{F,EL}$.

tion. At the start of Phase I, the MV contains the four-species reaction mixture to be separated. The MV both feeds the column and receives a side draw from it. Throughout this phase, the side draw has a higher concentration of ethyl lactate than the feed, thus driving the concentration of ethyl lactate in the MV toward the desired purity of 98 mol %. Ethanol and water are recovered in the distillate and sent to a pervaporation unit, where water is removed from the system, and the ethanol-rich retentate is recycled to the CSTR. Concentrated lactic acid is recovered in the bottoms of the column and recycled to the CSTR as well. Meanwhile, the CSTR is charged with an equimolar feed of fresh ethanol and lactic acid, and reaction proceeds in this new batch. Once the concentration of ethyl lactate in the MV reaches 98 mol %, Phase II begins. In this phase, the MV is drained and the product is collected. The column remains in operation, however, and continues to receive a feed from the MV and return a side draw to it. When the contents of the MV are nearly emptied, Phase III begins. In Phase III, the contents of the reactor, near chemical equilibrium, are transferred to the MV, while the column continues to operate. An animation of the SD process is available in the file, sd-animation1.mpeg in the Supplementary Material published with this article.[18] See the web address at http://www3.interscience.wiley.com/journal/120848573/suppinfo.

To control the distillation column, the following four degrees of freedom are available: the molar feed rate to the column (F_F), the side draw molar flow rate (F_S), the reflux ratio (R_{ref}), and the boilup ratio (R_{boil}). The latter two directly affect the composition profile of the column, whereas the former two affect the internal flow rates and cycle time. Because of the cyclic operating campaign, the tuning parameters vary from mode-to-mode during the cycle.

In Phase I, F_S is regulated with a model-based, feed-forward controller that follows the relationship:

$$F_S = F_F\, x_{F,EL} \tag{1}$$

where $x_{F,EL}$ is the mole fraction of ethyl lactate in the feed. Although this law is exact only when all of the ethyl lactate fed to the column is collected in a pure side draw, this reduces the ethyl lactate losses through the bottoms or distillate, causing ethyl lactate to concentrate rapidly in the middle vessel.

The reflux ratio is adjusted with a model-based, feed-forward, feedback controller to maximize the concentration of ethyl lactate in the side draw, $x_{S,EL}$. $x_{F,EL}$ and R_{boil} are the two key variables that affect the reflux ratio to achieve rapid separation. To develop the feed-forward model, a steady-state Aspen Plus 2004.1 simulation was developed using a RadFrac block with design variables equivalent to those used in the dynamic SD process (13 trays, feed above tray 6, side draw from tray 8, 1 bar pressure in the total condenser with $\Delta P = 0.01$ bar per stage). The flowsheet was simulated using a range of boilup ratios ($10 \le R_{boil} \le 25$) and feed compositions ($0.10 \le x_{F,EL} \le 0.95$). The molar ratios of the remaining three species in the feed were kept at $x_{F,W}/(1 - x_{F,EL}) = 0.46$, $x_{F,E}/(1 - x_{F,EL}) = 0.38$, and $x_{F,LA}/(1 - x_{F,EL}) = 0.16$, which are approximately their molar ratios at chemical equilibrium at 95°C. This assumes that throughout the separation process, water, ethanol, and lactic acid exit the middle vessel in the same ethyl lactate-free composition. For each simulation, R_{ref} was optimized to maximize $x_{S,EL}$, the ethyl lactate mole fraction in the side draw. F_S was fixed according to Eq. 1. This optimization problem has a maximum because when R_{ref} is too high, water moves down the column and appears in the side draw, lowering the amount of ethyl lactate. Alternatively, when R_{ref} is too low, more lactic acid appears in the side draw. The results, shown in Figure 5, indicate that for a given feed composition, the optimal R_{ref} varies linearly with R_{boil}. The slopes and intercepts of these linear relationships are plotted in Figure 6, showing that the slopes and intercepts themselves are approximately linear functions of $x_{F,EL}$. However, an abrupt shift in slope occurs at $x_{F,EL} = 0.6$, possibly due to a bifurcation with multiple steady states in the column for feeds above $x_{F,EL} = 0.6$. Consequently, multiple modes are implemented during Phase I, depending on $x_{F,EL}$, with the feed-forward model:

$$R_{ref} = \begin{cases} (-0.0796 x_{F,EL} + 0.3069) R_{boil} \\ \quad + (-0.8281 x_{F,EL} - 1.1393) & x_{F,EL} < 0.6 \\ (-0.5079 x_{F,EL} + 0.5621) R_{boil} \\ \quad + (7.661 x_{F,EL} - 6.4184) & x_{F,EL} \ge 0.6 \end{cases} \tag{2}$$

For the feedback controller, simple proportional control is adequate, with a target setpoint of $x_{S,EL} = 0.99$. Thus, the estimate for R_{ref} from Eq. 2 is added to the proportional gain times the error in $x_{S,EL}$ ($e_{S,EL}$), as shown in Table 1. Note that R_{ref} is subject to a maximum, $R_{ref,max}$, as indicated in Table 8.

To improve the performance of the column, a PI feedback controller is added at the bottom, with R_{boil} adjusted to give $x_{B,EL} = 0.01$, as indicated in Table 1. The combination provides better performance when the tuning parameters for the PI controller are specific to each mode, as shown in Table 8. Note that R_{boil} is subject to a maximum. This reduces the ethyl lactate recycled to the CSTR, while circumventing high boilup ratios that move ethyl lactate into the distillate. Performance is further improved with another set of tuning parameters when $x_{F,EL}$ exceeds 0.80. Therefore, Phase I involves the following three modes: Mode 1 ($x_{F,EL} < 0.6$), Mode 2 ($0.6 \leq x_{F,EL} < 0.8$), and Mode 3 ($0.8 \leq x_{F,EL} < 0.98$).

F_F is regulated through a feed-forward, model-based controller designed to keep the liquid and vapor flow rates inside the column balanced to prevent weeping and flooding, by satisfying the constraint:

$$D - 0.1524 \text{ m} \leq D_{min}(t) \leq D \tag{3}$$

where D is the specified diameter of the column in m and D_{min} is the minimum diameter to prevent flooding, as calculated by the Fair correlation[19]. To achieve this, F_F tracks a polynomial function of $x_{F,EL}$ where the coefficients of the polynomial are different for each mode and design. The functions are summarized in Table 1 and expressed explicitly in Table 8.

In Phase II (Mode 4) and Phase III (Mode 5), F_F, F_S, R_{ref}, and R_{boil} are held constant. A complete summary of the controller arrangements can be found in Table 1.

The dynamics of the column and MV were simulated using the method of Adams and Seider.[10] The physical properties, chemical reaction, and pervaporation components were simulated using the methods described in the next section.

Table 1. SD Control System Summary

	I			II	III
	1	2	3	4	5
F_F	$F_F = f_{F,1}(x_{F,EL})$	$F_F = f_{F,2}(x_{F,EL})$	$F_F = f_{F,3}(x_{F,EL})$	$F_F = c_{F,4}$	$F_F = c_{F,5}$
F_S	$F_S = F_F x_{F,EL}$	$F_S = F_F x_{F,EL}$	$F_S = F_F x_{F,EL}$	$F_S = c_{S,4}$	$F_S = c_{S,5}$
R_{boil}	$\Delta R_{boil} = Kc_{boil,1}(e_{B,EL})$	$\Delta R_{boil} = Kc_{boil,2} \times (e_{B,EL} + \tau_{1,2}^{-1}\int e_{B,EL}dt)$	$\Delta R_{boil} = Kc_{boil,3} \times (e_{B,EL} + \tau_{1,3}^{-1}\int e_{B,EL}dt)$	$R_{boil} = c_{boil,4}$	$R_{boil} = c_{boil,5}$
R_{ref}	$R_{ref} = f_{ref,1}(x_{F,EL},R_{boil}) + Kc_{ref,1}(e_{S,EL})$	$R_{ref} = f_{ref,2}(x_{F,EL},R_{boil}) + Kc_{ref,2}(e_{S,EL})$	$R_{ref} = f_{ref,3}(x_{F,EL},R_{boil}) + Kc_{ref,3}(e_{S,EL})$	$R_{ref} = c_{ref,4}$	$R_{ref} = c_{ref,5}$
Stop trigger	$x_{F,EL} \geq 0.6$	$x_{F,EL} \geq 0.8$	$x_{F,EL} \geq 0.98$	$V_{MV} \leq 5L$	$V_{CSTR} \leq 15L$

I, II, and III are the phases, and 1, 2, 3, 4, and 5 are the modes.
$e = x - x_{Sp}$, which is the deviation of the mole fraction from its setpoint. Kc, τ_I, and c are constants which vary for each mode (see Table 8). f_{ref} and f_F are functions that vary for each mode (see Table 8). The end condition for each mode is also shown. V_{MV} and V_{CSTR} are the volumes of the MV and CSTR, respectively.

Model Development

Chemical reaction

The exothermic, reversible reaction in this case study is shown in Figure 1. A well-known, low-boiling azeotrope between ethanol and water exists at about 78°C. The heat of reaction, determined using the RSTOIC block in Aspen Plus 2004.1, is −787.73 J/mol ethanol at 95°C. The reaction rate, derived from heterogeneous esterification experiments,[14] is:

$$r_{EL} = \frac{k(C_E C_{LA} - C_W C_{EL}/K)}{C_E + aC_W C_{EL}} \tag{4}$$

where k is the rate constant (min^{-1}), C is the concentration (kmol/L) of ethanol, lactic acid, water, or ethyl lactate, r_{EL} is the intrinsic rate of reaction of ethyl lactate [kmol/(L min)], K is the equilibrium constant for the esterification reaction, and a is a temperature dependent constant (L/kmol) given by:

Table 2. Constants in Reaction Equations

Variable	Value
ΔH_A (kJ/mol)	−38.37
E (kJ/mol)	30.54
g_0 (kJ/mol)	−4.433
g_1 [kJ/(mol K)]	3.550×10^{-3}
k_{A0} (L/kmol)	2.02×10^{-3}
k_0 [L/(kg min)]	1.257×10^{4}
w_{cat} (kg/kg)	0.04

Table 3. UNIQUAC Constants used in Aspen Plus and BatchSep Simulations

Species i	Species j	A_{ij}	A_{ji}	B_{ij} (K)	B_{ji} (K)
Ethanol	Water	2.0046	−2.4936	−728.97	756.95
Ethanol	Ethyl lactate			−30.472	−6.774
Ethanol	Lactic acid			51.185	−87.947
Water	Ethyl lactate			−282.03	131.31
Ethyl lactate	Lactic acid			148.785	−196.962
Lactic acid	Water			357.47	−499.38

$$a = (K_{A0}/K)\exp(-\Delta H_A/RT) \tag{5}$$

where R is the universal gas constant [kJ/(mol K)], and T is the temperature of the reaction (K). K_{A0} (L/kmol) and ΔH_A (kJ/mol) are the pre-exponential factor for the adsorption equilibrium constant and the heat of adsorption, respectively, for the adsorption reaction, A + S ↔ AS, where A is lactic acid and S is a catalytically active site. These constants were determined by Benedict et al. by regression of experimental data.[14] The esterification equilibrium constant follows the relationship:

$$K = \exp(-\Delta G^\circ/RT) \tag{6}$$

where $-\Delta G^\circ$ (kJ/mol) is the Gibbs free energy of reaction in the standard state, a function of temperature:

$$-\Delta G^\circ = -(g_1 T + g_0) \tag{7}$$

where g_0 (kJ/mol) and g_1 [kJ/(mol K)] were determined by regression of data published in Benedict et al.[14] The rate constant is dependent on temperature and catalyst weight, according to:

$$k = \rho_{liq} w_{cat} k_o \exp(-E/RT) \tag{8}$$

where ρ_{liq} is the density of the liquid (kg/L), w_{cat} is the weight ratio of catalyst to liquid (kg of Amberlyst XN-1010 per kg of solution), k_0 is the rate constant coefficient [L/(kg min)], and E is the activation energy [kJ/(mol K)]. The values of the parameters in Eqs. 5–8 are provided in Table 2.

Chemical properties

The Aspen Properties 2004.1 engine is used to determine the densities, surface tensions, vapor–liquid equilibria (VLE), activity coefficients, and other physical properties for all simulations in this case study. The VLE were modeled with the UNIQUAC method, using coefficients determined from experimental data for the ethanol–ethyl lactate binary pair[20] and the water–ethyl lactate binary pair,[12] at atmospheric pressure. The experimental and UNIQUAC predicted VLE values were in close agreement. The remaining UNIQUAC coefficients were either taken from the Aspen Properties 2004.1 VLE-IG and LLE-LIT databases or predicted using the UNIFAC group contribution methods, as shown in Table 3.

Pervaporation

Although steady state models for pervaporation are prevalent, dynamic models are still in the early stages of development. These models require large amounts of computational effort to describe the dynamics and are unsuitable for application in a plant-level dynamic simulation.[21,22] One dynamic pervaporation model showed that after a large step change in the input, steady state can be reached in as little as 2 min.[23] This small transition time, which is several orders of magnitude less than the run time of a batch or semicontinuous cycle, indicates that a pseudo-steady state (PSS) model adequately describes the dynamics while requiring a small fraction of the computational effort. Consequently, a PSS model is used herein with the partial-pressure difference across the membrane as the driving force for membrane separation,[24] as shown schematically in Figure 7.

The dynamic model equations for pervaporation are as follows:

$$m_P w_{P,i} = \overline{P}_i A_m (\gamma_{F,i} x_{F,i} P^*_{F,i} - P_P y_{P,i}) \tag{9}$$

where m_P is the mass flow of the permeate (kg/min), $w_{P,i}$ is the mass fraction of species i in the permeate, $\overline{P}_i$ is the

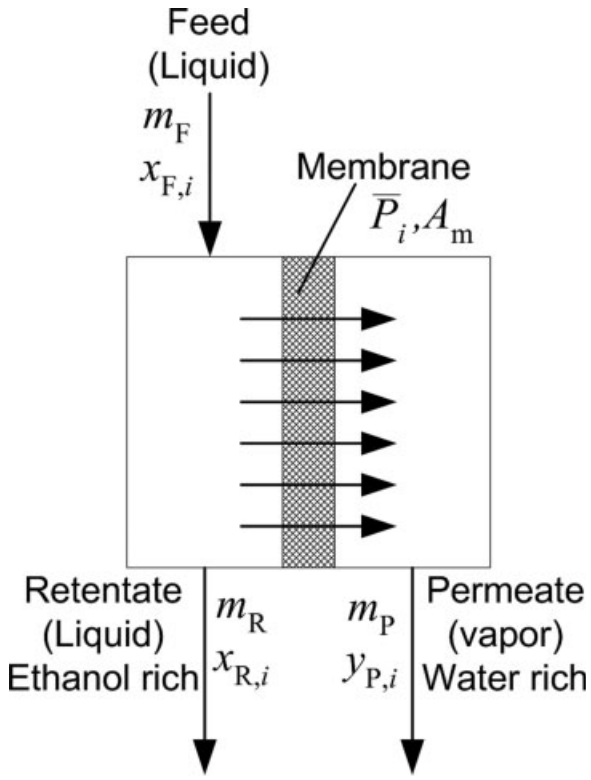

Figure 7. PSS model for pervaporation.

permeance of species i through the membrane [kg/(m^2 min bar)], A_m is the membrane transfer-surface area (m^2), $\gamma_{F,i}$ is the activity coefficient of species i in the feed, $x_{F,i}$ is the mole fraction of species i in the feed, $P^*_{F,i}$ is the vapor pressure of species i in the feed (bar), P_P is the permeate pressure (bar), and $y_{P,i}$ is the mole fraction of species i in the permeate. For simplicity in solving, $w_{P,i}$ can be expressed in terms of $y_{P,i}$ as follows:

$$w_{P,i} = \left(\frac{y_{P,i}\mathrm{MW}_i}{\sum_{j=1}^{N} y_{P,j}\mathrm{MW}_j} \right) \tag{10}$$

where N is the total number of species and MW_i is the molecular weight of species i. The mole fractions follow the unity-summation relationship:

$$\sum_{i=1}^{N} y_{P,i} = 1 \tag{11}$$

For a given time step, Eqs. 9–11 form a system of $N + 1$ equations in $N + 1$ unknowns, which is expressed in vector notation as:

$$\underline{f}(\underline{z}) = 0 = \begin{bmatrix} \overline{P}_i A_m \left(\sum_{j=1}^{N} z_j \mathrm{MW}_j \right) \left(\gamma_{F,i} x_{F,i} P^*_{F,i} - P_P z_i \right) - z_{N+1} z_i \mathrm{MW}_i & \text{rows } i = 1, \ldots, N \\ \sum_{j=1}^{N} z_j - 1 & \text{row } i = N+1 \end{bmatrix} \tag{12}$$

where $\underline{z}$ is an $(N + 1) \times 1$ vector:

$$\underline{z} := \begin{bmatrix} y_{P,1} & \ldots & y_{P,N} & m_P \end{bmatrix}^T$$

Equation (12) is solved using the Newton–Raphson method:

$$\underline{f}(\underline{z} + \Delta\underline{z}) = \underline{f}(\underline{z}) + \underline{\underline{J}}\Delta\underline{z} \tag{13}$$

where the elements of $\underline{\underline{J}}$, the Jacobian matrix, are as follows:

$$J_{i,k} = \frac{\partial f_i}{\partial z_k} = \overline{P}_i A_m \left(\gamma_{F,i} x_{F,i} P^*_{F,i} \mathrm{MW}_k - P_P \left(z_i \mathrm{MW}_k + \delta^k_i \sum_{j=1}^{N} z_j \mathrm{MW}_j \right) \right) - \delta^k_i z_{N+1} \mathrm{MW}_k \quad \text{for all } i = 1, \ldots, N, k = 1, \ldots, N \tag{14}$$

$$J_{N+1,k} = \frac{\partial f_{N+1}}{\partial z_k} = 1 \quad \text{for all } k = 1, \ldots, N \tag{15}$$

$$J_{i,N+1} = \frac{\partial f_i}{\partial z_{N+1}} = -z_i \mathrm{MW}_i \quad \text{for all } i = 1, \ldots, N \tag{16}$$

$$J_{N+1,N+1} = \frac{\partial f_{N+1}}{\partial z_{N+1}} = 0 \tag{17}$$

where δ^k_i is the Kroeneker delta function ($\delta^k_i = 0$, $i \neq k$; $\delta^k_i = 1$, $i = k$). With the PSS assumption, there is no holdup inside the pervaporation unit. Therefore, the dynamic mole balances are given as:

$$m_F = m_R + m_P \tag{18}$$

$$m_F w_{F,i} = m_R w_{R,i} + m_P w_{P,i} \quad \text{for all } i = 1, \ldots, N \tag{19}$$

where m_F and m_R are the mass flow rates (kg/min) of the feed and retentate, respectively; and $w_{R,i}$ and $w_{P,i}$ are the mass fractions of species i in the retentate and permeate, respectively. At each time step, after Eq. 12 is solved, Eqs. 18 and 19 are solved to determine the flow rate and mass fractions of the retentate.

Data for $\overline{P}_i$ are based on experimentally determined values using a hydrophilic, multilayer, mixed-matrix membrane known as MMMM-20. The data published in Guan et al.[25] were regressed and described as follows:

$$\overline{P}_E = \begin{cases} (b_{E1} w_{F,E} + b_{E2} w^2_{F,E}) \exp(-E_E/RT) & \text{for } w_{F,E} \geq 0.1 \\ \overline{P}_E\{0.1\}(w_{F,E}/0.1) & \text{for } w_{F,E} < 0.1 \end{cases} \tag{20}$$

$$\overline{P}_W = \begin{cases} b_{W0} \exp(b_{W1} w_{F,W}) \exp(-E_W/RT) & \text{for } w_{F,W} \geq 0.1 \\ \overline{P}_W\{0.1\}(w_{F,W}/0.1) & \text{for } w_{F,W} < 0.1 \end{cases} \tag{21}$$

where b_{E1}, b_{E2}, b_{W0}, b_{W1}, E_E, and E_W are coefficients in Table 4. No data were available for the permeation of ethyl lactate or lactic acid through this membrane. However, their permeation rates are neglected because they appear in the pervaporation feed in small amounts. Furthermore, they are larger molecules than ethanol and water and have slower permeation rates through the pores of the hydrophilic membrane. Consequently, the permeance values for ethyl lactate and lactic acid are assumed to be zero.

Results

Continuous process

For the continuous process, using the conditions in Figure 1 and Table 5, the first column achieves an excellent separation with less than 0.1% ethyl lactate in the distillate and less than 0.2% water in the bottoms using $R_{ref} = 13.0$, $R_{boil} = 11.5$, saturated liquid feed above tray 6 (numbered from the top), and 1 bar pressure in the condenser with $\Delta P = 0.01$ bar per tray. In the second column, ethyl lactate and lactic acid are separated at 98–99% purity using $R_{ref} = 0.3$, $R_{boil} = 1.7$, saturated

Table 4. Constants in the Pervaporation Model

Variable	Value
b_{E1} [kg/(m^2 min bar)]	3.1466×10^6
b_{E2} [kg/(m^2 min bar)]	-3.4354×10^6
b_{W0} [kg/(m^2 min bar)]	0.42567
b_{W1}	3.1784
E_E (kJ/mol)	59.11
E_W (kJ/mol)	10.12

Table 5. Summary of Continuous Process Variables for Selected Cases

Property\Case	1	2	3	4	5	6
EL production (MMkg/yr)	0.19	0.88	1.77	2.65	3.98	4.86
E/W Removal Column						
Diameter (m [ft])	0.305 [1.0]	0.457 [1.5]	0.610 [2.0]	0.762 [2.5]	0.914 [3.0]	1.07 [3.5]
Reboiler Duty (GJ/h)	0.177	0.887	1.775	2.662	3.993	4.880
Condenser Duty (GJ/h)	0.171	0.854	1.708	2.562	3.842	4.696
Total Direct Cost ($)	355,300	355,300	414,700	463,100	506,000	619,300
EL Removal Column						
Diameter (m [ft])	0.305 [1.0]	0.305 [1.0]	0.305 [1.0]	0.305 [1.0]	0.305 [1.0]	0.305 [1.0]
Reboiler Duty (GJ/h)	0.012	0.061	0.121	0.182	0.272	0.332
Condenser Duty (GJ/h)	0.012	0.058	0.117	0.175	0.263	0.322
Total Direct Cost ($)	425,200	425,200	425,200	425,200	425,200	425,200
PFR						
Volume (L)	170	852	1,703	2,551	3,831	4,683
Total Direct Cost ($)	127,000	185,600	216,900	258,500	304,100	320,800
Pervaporation Unit						
Membrane Area (m^2)	8	30	60	100	135	165
Total Direct Cost ($)	2,600	9,700	19,400	32,400	43,700	53,400
Condensers						
E/W Condenser Area (m^2)	0.7	3.4	7.0	10.4	15.6	19.0
EL Condenser Area (m^2)	0.09	0.3	0.6	0.8	1.2	1.5
Tot. Dir. Cost Condensers ($)	161,200	161,200	161,200	161,200	179,000	200,200
Reboilers						
EL/LA Reboiler Area (m^2)	0.4	1.9	3.7	5.6	8.4	10.3
LA Reboiler Area (m^2)	0.1	0.2	0.5	0.7	1.0	1.3
Tot. Dir. Cost Reboilers ($)	230,500	230,500	233,300	242,100	254,500	258,500
Cost Summary						
Total Manufacturing ($1,000/yr)	811	876	963	1,050	1,180	1,280
Total Capital ($1,000)	1,980	2,080	2,240	2,410	2,600	2,850
Total Lifetime ($1,000)	4,410	4,710	5,120	5,560	6,130	6,690

liquid feed above tray 5, and the pressure conditions in the first column. The sizes of the condensers, reboilers, and pervaporation unit varied with the throughput. For the PFR, the volume needed to achieve the conversion is[26] given as:

$$V_{\mathrm{PFR}} = F_{\mathrm{F,E}} \int_0^{x_{\mathrm{eq}}} \frac{dx}{r_{\mathrm{EL}}} \tag{22}$$

where V_{PFR} is the volume of the PFR (L), $F_{\mathrm{F,E}}$ is the molar flow rate of ethanol in the feed (kmol/min), x_{eq} is the equilibrium conversion using Eq. 6, and r_{EL} is defined by Eq. 4. The temperature, T, determines x_{eq}, the total heat of reaction, and the associated costs of cooling the reactor. Higher temperatures yield lower conversions, but require smaller, less costly reactors. Thus, T is varied to minimize the total cost of cooling and the capital expenses of the reactor per mole of ethyl lactate produced. To prevent vaporization, the maximum T allowed is 95°C, since the bubble point of the reaction mixture is 97°C at atmospheric pressure. Because x_{eq} does not vary significantly with T, as shown in Figure 8, higher temperatures significantly reduce the capital cost of the reactor without much loss of conversion. Thus, the highest safe temperature of 95°C is the most economic choice. Note that a PFR is advantageous for continuous systems because the same conversion can be achieved with a fraction of the volume required by a CSTR. For example, for Case 6, the required PFR volume at 95°C is 4683 L (including the catalyst volume), while a CSTR requires approximately 4.16×10^5 L. A summary of the key process variables is in Table 5.

Batch process

The batch process specifications are varied to achieve the shortest batch cycle time for a variety of batch charge sizes. A small column [0.305 m (1 ft) diameter, 5 trays] is sufficient and permits shorter cycle times due to low tray holdups. The batch size and heat flux are varied to minimize the total lifetime cost for a given production rate. For production rates above 0.5 MM kg/yr of ethyl lactate, because the jacket and coils in the pot are insufficient to provide the high heat flux required, a side heating unit is used. To achieve a higher

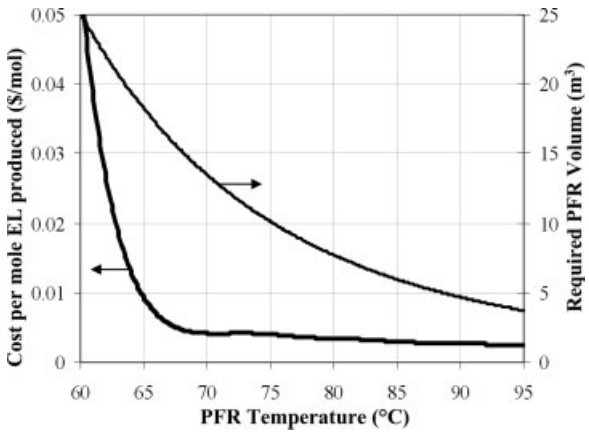

Figure 8. Required PFR volume and production cost per kmol ethyl lactate produced as a function of reactor temperature.

Table 6. Batch Recipe

Mode	Description	Actions	Stopping Criteria
1	Charge Pot	Transfer CSTR contents (E,EL,W,LA) to pot.	CSTR emptied
2	Collect E&W	Begin heating with medium pressure steam. Transfer Tank 1 contents (LA) to CSTR. Collect ethanol and water in distillate, send to Tank 2. Maintain $x_{D,EL} < 0.001$ with reflux controller. Slowly send Tank 2 contents to pervaporation unit. Recycle ethanol retentate to CSTR.	$x_{D,W} > 0.99$
3	Collect W	Collect water in distillate.	$x_{D,W} < 0.95$
4	Transition to EL in Distillate	Send off-spec distillate to downstream recovery. Switch to high-pressure steam. Change reflux controller setpoint to maintain $x_{D,EL} > 0.98$.	$x_{D,EL} > 0.98$
5	Collect EL	Send on-spec distillate downstream.	$x_{Pot,LA} > 0.97$
6	Cool Down	Stop heating. Liquid in column falls into pot.	2 h elapsed
7	Recover LA	Transfer pot contents (LA) to Tank 1.	Pot emptied

conversion in the reactor of 66%, the CSTR temperature is fixed at 25°C. The kinetics at this temperature are slow, but are not the bottleneck during the long cycle times. The final batch recipe is in Table 6, and a summary of the variables for different capacities is in Table 7.

Semicontinuous process

The SD process was simulated using a variety of production capacities and specifications. The capacity of the process is most readily increased by increasing the feed and side draw rates, thereby increasing the flow rates inside the column. This, however, requires larger column diameters to operate without weeping and flooding. For each case study, the column diameter is selected from the range 0.46 m (1.5 ft) to 1.37 m (4.5 ft) in 0.3 m (0.5 ft) increments, and then the control system is tuned to satisfy Eq. 3 throughout the cycle while minimizing the total lifetime cost. For this study, a three-year lifetime is assumed, which is consistent with many specialty chemical operations. Figure 9 shows an example of D_{min} remaining within this range during the course of the cycle, noting that the column diameter in the top section (above the feed on Tray 5, starting at the top) and the bottom section, are different.

Throughout the cycle, the ethanol, water, and lactic acid holdup inside the MV gradually decreases, whereas the ethyl

Table 7. Batch Cost Summary for Selected Cases

Property\Case	1	2	3	4	5	6
EL production (MMkg/yr)	0.06	0.35	0.41	0.48	0.65	0.94
Distillation Column						
Diameter (m [ft])	0.305 [1.0]	0.305 [1.0]	0.305 [1.0]	0.305 [1.0]	0.305 [1.0]	0.305 [1.0]
Pot Heating Duty (GJ/cycle)	8.5	10.7	30.8	179.7	22.2	21.7
Condenser Duty (GJ/cycle)	8.3	10.6	30.6	179	86.7	64.7
Total Direct Cost ($)	261,000	261,000	261,000	261,000	261,000	261,000
CSTR						
Volume (L)	1,360	2,450	4,880	14,600	4,880	4,850
Total Direct Cost ($)	255,500	291,900	388,500	710,900	388,500	387,900
Pervaporation Unit						
Membrane Area (m^2)	8.0	8.0	8.0	8.0	15	15
Total Direct Cost ($)	2,590	2,590	2,590	2,590	4,860	4,860
Condenser						
Condenser Area (m^2)	39.6	89.2	122	223	111	126
Total Direct Cost ($)	76,600	94,400	113,500	142,600	111,900	113,700
Side Heating Reboiler						
Reboiler Area (m^2)	N/A	N/A	N/A	N/A	48.0	48.0
Total Direct Cost ($)					138,700	138,700
Tanks and Vessels						
Pot (L)	1,170	2,520	4,430	13,300	4,430*	4,430*
Tank 1 (L)	151	333	712	2,230	712	697
Tank 2 (L)	496	916	1,772	5,300	1,740	1,711
Total Direct Cost ($)	282,700	330,000	380,700	620,600	358,700	358,600
Batch Performance						
Cycle Time (min)	3,345	1,309	2,474	6,635	1,499	983
Ethyl Lac. Produced (kmol/cyc.)	3.58	8.76	18.63	57.50	18.80	18.36
Cost Summary						
Total Manufacturing ($1,000/yr)	716	762	825	1,050	2,740	3,570
Total Capital ($1,000)	1,440	1,600	1,880	2,850	2,090	2,090
Total Lifetime ($1,000)	3,580	3,890	4,360	5,990	10,310	12,800

*A side heating vessel was used, so the pot did not have a heating jacket or coils.

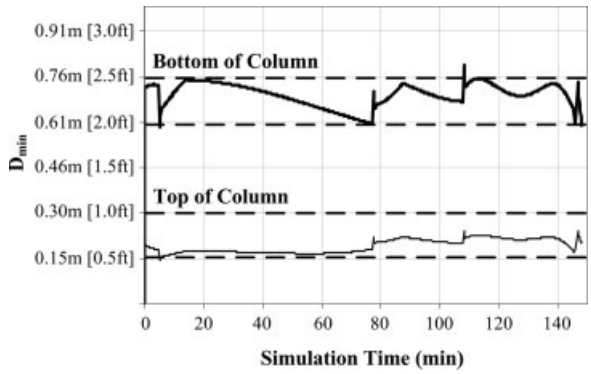

Figure 9. The minimum column diameter to prevent flooding—0.76 m (2.5 ft) column diameter below the feed tray.

lactate holdup remains approximately constant, as shown in Figure 10. Because the feed composition decreases in ethanol, water, and lactic acid over the course of the cycle, the flow rates of the distillate and bottoms, as shown in Figure 11, must decrease as well to prevent ethyl lactate from leaving through either of these streams. Likewise, the feed flow rate must increase to prevent weeping and flooding. Because the internal flow rates are relatively constant whereas the distillate and bottom streams decrease as the cycle progresses, the reflux and boilup ratios must therefore increase, as shown in Figure 12. Even though very high ratios are reached, this is not unreasonable since the distillate and bottoms flow rates become very small.

The control system achieves 98% ethyl lactate purity in the MV for each case. The lactic acid concentration in the bottoms gradually achieves high concentration near the end of the cycle as shown in Figure 13, and the distillate remains free of ethyl lactate for most of the cycle, as shown in Figure 14. The internal liquid mole fraction profile of the column also remains stable throughout the cycle, showing little change despite the rapidly changing feed composition and reflux and boilup ratios. The profile for one case is shown in Figure 15. An animation showing the dynamics of the column profile over the course of the cycle is available in the file, sd-animation2.mpeg in the Supplementary Material published with this article.[27] See the web address at http://www3.interscience.wiley.com/journal/120848573/suppinfo. The final tuning parameters used for each case can be found in Table 8.

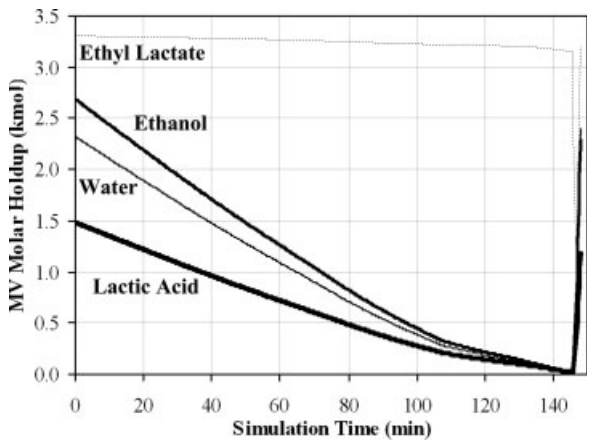

Figure 10. Molar holdups in the MV—0.76 m (2.5 ft) column diameter below the feed tray.

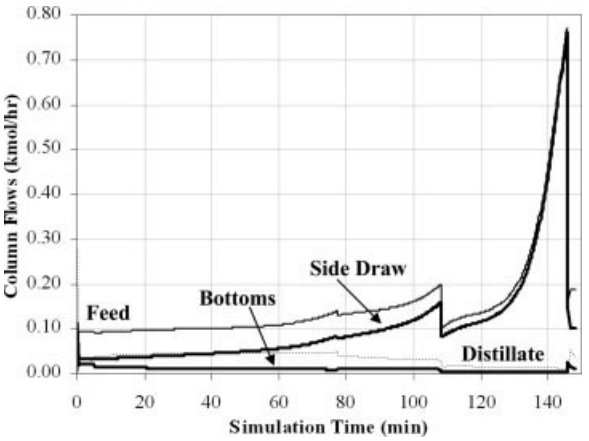

Figure 11. Flow rates of the feed, side draw, bottoms, and distillate—0.76 m (2.5 ft) column diameter below the feed tray.

The batch size also has a significant effect on the total lifetime cost. For example, doubling the batch size nearly doubles the cycle time required to process it, but produces twice as much per cycle, leaving the yearly production rate relatively unchanged. Larger batches are more thermodynamically efficient because a smaller percentage of the cycle time is spent transitioning the column during the transient parts of the cycle. However, this effect is small, and consequently, smaller batch sizes are economically preferred in general. In this study, a batch size of about 757 L (200 gal) is preferred when using column diameters below 1.37 m (4.5 ft) and 2271 L (600 gal) for larger columns. Because of the short cycle times, fast kinetics is needed in the reactor, and consequently, the CSTR temperature is set at 95°C. Since the bubble point of the mixture at atmospheric pressure is as low as 97°C, 95°C is the maximum safe operating temperature. A summary of the design parameters and costs for several case studies can be found in Table 9.

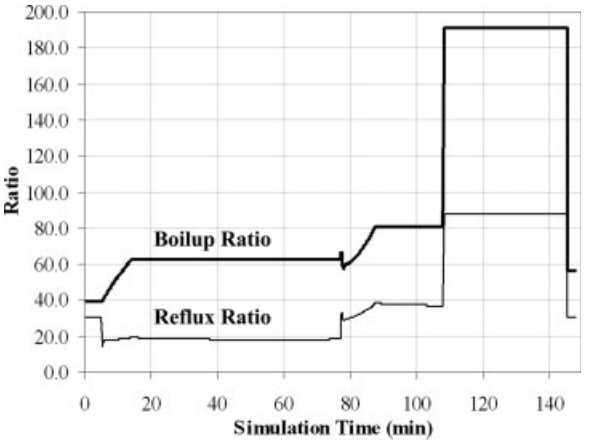

Figure 12. Reflux and boilup ratios—0.76 m (2.5 ft) column diameter below the feed tray.

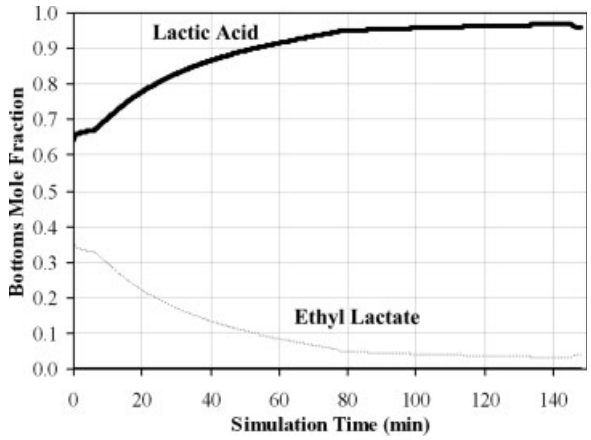

Figure 13. Bottoms composition—0.76 m (2.5 ft) column diameter below the feed tray.

Economics

For each case study, Aspen Icarus Process Evaluator 2004.1 is used to estimate the total direct cost (which includes platforms, ladders, piping, instrumentation, paint, and others) of the distillation columns, tanks, condensers, reboilers, and reactors. For the equipment used in this study, the Aspen IPE cost estimates vary monotonically with key size variables. No abrupt changes are encountered that often accompany unreasonable extrapolations. Also, to avoid such extrapolations, ethyl lactate throughputs below 0.05 MM kg/yr were avoided, and column diameters below 1.0 ft were not used. Note that the CSTR, reboilers, columns, and tanks that encounter significant amounts of lactic acid (>2% concentration) are fabricated with monel, an acid-resistant alloy. The remaining process equipment uses carbon steel. The distillation columns are assumed to have 70% tray efficiency. The catalyst cost is assumed to be \$67.08 kg^{-1} of Amberlyst-15, a typical acid catalyst.[28] However, this was a negligible contribution (<1%) to the reported total direct cost of the CSTRs. The purchase cost of the pervaporation units is estimated at \$322.92 per m^2 of membrane surface area (see Ref. 29; p. 554). The total direct cost is estimated by multiplying the purchase cost by a bare-module factor (see Ref. 29; p. 490); of 3.3. The cost of steam (see Ref. 29; p. 802); at 148, 186, and 273°C is taken to be \$5.5, \$8.8, and \$12.1 per 1000 kg, respectively. Cooling water at 8 and 30°C are priced at \$3.3 and \$0.3095 per GJ of cooling load, respectively. The cost of pumps is neglected due to their insignificant contribution to the total cost. For the columns, a tray efficiency of 70% is assumed.

Control costs are difficult to estimate accurately at this stage of the design process. Herein, the estimated costs of controllers, transmitters, and valves provided by Aspen IPE for a default P&ID are used. These are included in the total direct cost for each piece of equipment. Although the control configurations for the semicontinuous and batch processes differ from that used by Aspen IPE, the number and type of controllers, transmitters, and valves for each equipment item do not differ significantly. Consequently, it is assumed that the differential costs are negligible. Labor costs assume that one operator is sufficient for each process (batch, semicontinuous, or continuous), at \$30 hr^{-1} of direct wages. Maintenance and overhead costs are based on the equations in Seider et al. (see Ref. 29; p. 566). Although the batch and semicontinuous processes are more complex, about half as much equipment is monitored and serviced. Consequently, the numbers of operator-hours to supervise batch, semicontinuous, and continuous processes are assumed to be comparable. For each case study, the total lifetime cost is computed using operations over 3 years (from start of production to completion), including labor, maintenance, land, taxes, overhead, and operations. All costs are based on the dollar value in the first quarter of 2006.

As expected, the annual manufacturing costs of the continuous system are lower than the others for high capacities as shown in Figure 16 and had a smaller slope. The SD and batch processes require the least energy expenditure at the low ends of the capacity range tested, with SD requiring the least energy expense for capacities between about 0.3 and 1.0 MM kg/yr of ethyl lactate. The SD process also requires the least capital expenses for the entire production range tested, as shown in Figure 17. When compared with the continuous process, less capital is required because only one dis-

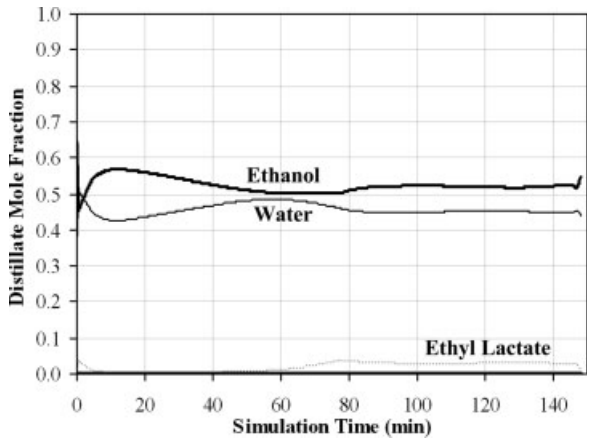

Figure 14. Distillate mole fractions—0.76 m (2.5 ft) column diameter below the feed tray.

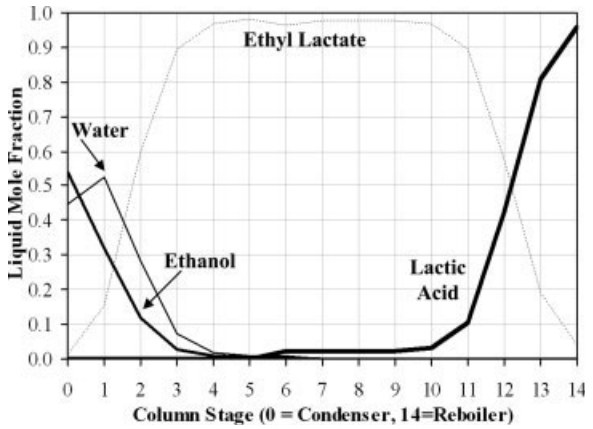

Figure 15. Column liquid mole fraction profile near the end of the cycle—0.76 m (2.5 ft) column diameter below the feed tray.

Table 8. Final Tuning Parameters of Four SD Cases

Parameter	0.457 m (1.5 ft)	0.762 m (2.5 ft)	1.07 m (3.5 ft)	1.22 m (4.0 ft)
$f_{F,1}(x_{F,EL})$*	$0.245 - 1.38x + 2.76x^2 - 1.65x^3$	$-0.477 + 3.85x - 8.68x^2 + 6.63x^3$	$0.481 - 0.454x - 2.47x^2 + 4.57x^3$	$0.558 - 0.454x - 2.47x^2 + 4.57x^3$
$f_{F,2}(x_{F,EL})$*	$-1.52 + 7.05x - 10.6x^2 + 5.36x^3$	$-3.22 + 15.2x - 23.2x^2 + 11.9x^3$	$5.93 - 24.0x + 32.0x^2 - 13.3x^3$	$5.98 - 24.0x + 32.0x^2 - 13.3x^3$
$f_{F,3}(x_{F,EL})$*	$-40.5 + 147.9x - 179.9x^2 + 72.9x^3$	$-133 + 476x - 565x^2 + 224x^3$	$-207 + 759x - 928x^2 + 378x^3$	$-270 + 975x - 1{,}173x^2 + 471x^3$
$[c_{F,4}, c_{F,5}]$*	[0.140, 0.131]	[0.16, 0.190]	[0.319, 0.267]	[0.419, 0.267]
$[c_{S,4}, c_{S,5}]$*	[0.110, 0.010]	[0.146, 0.100]	[0.266, 0.116]	[0.366, 0.116]
$Kc_{boil,i}$†	[−2.36, −3.91, −29.9]	[−0.456, −8.51, −1,230]	[−0.456, −8.51, −29.9]	[−0.456, −8.51, −29.9]
$[\tau_{I,2}, \tau_{I,3}]$	[∞, 50]	[10, 50]	[10, 50]	[10, 50]
$R_{ref,max,i}$†	[25, 50, 71]	[25, 40, 88]	[25, 40, 88]	[25, 40, 110]
$R_{boil,max,i}$†	[63, 80, 191]	[63, 81, 191]	[72, 81, 191]	[72, 81, 191]
$[c_{boil,4}, c_{boil,5}]$	[6.7, 2.2]	[23.9, 56.1]	[23.9, 56.1]	[33.9, 56.1]
$f_{ref,i}$	See Eq. 2	See Eq. 2	See Eq. 2	See Eq. 2
$Kc_{ref,i}$ i = [1,2,3]	[1,500, 1,500, 3,300]	[750, 6, 957]	[406, 6, 957]	[406, 6, 957]
$[c_{ref,4}, c_{ref,5}]$	[419, 41.2]	[334, 30.9]	[334, 30.9]	[334, 30.9]

*Units are kmol/min.
†For i = [1,2,3].

tillation column, condenser, and reboiler are required. As capacity increases, the total capital cost of the two systems increases at about the same rate.

When compared with batch, the batch system has slightly higher capital costs than the SD system for low capacities. This is largely attributed to the large condenser needed to achieve 98% ethyl lactate purity during Mode 5 of the batch system. Capacity increases are achieved by increasing the size of the process vessels and/or the pot heating duty. Because the process vessels are mostly high-cost monel, the capital costs increase rapidly when the process vessel size is increased. Also, when pot heating is increased, manufacturing costs increase rapidly because high pressure steam is required due to the high boiling point of the mixture throughout the cycle. Thus, the costs increase rapidly with capacity. For capacities greater than 0.5 MM kg/yr, it is less expensive

Table 9. SD Cost Summary for Selected Cases

Property\Case	1	2	3	4	5	6
EL production (MMkg/yr)	0.44	0.74	1.20	1.61	2.18	2.71
Distillation Column						
Diameter at Top (m [ft])	0.152 [0.5]	0.152 [0.5]	0.305 [1.0]	0.305 [1.0]	0.305 [1.0]	0.305 [1.0]
Diameter at Bottom (m [ft])	0.457 [1.5]	0.610 [2.0]	0.762 [2.5]	0.914 [3.0]	1.07 [3.5]	1.22 [4.0]
Reboiler Heating Duty (GJ/cyc.)	7.113	7.796	7.478	8.356	7.914	7.914
Condenser Duty (GJ/cycle)	6.872	7.611	7.700	8.122	7.745	7.832
Total Direct Cost ($)	246,200	327,600	334,100	365,800	450,300	476,700
CSTR						
Volume (L)	943	935	927	920	912	912
Total Direct Cost ($)	252,200	252,000	251,900	251,800	251,800	251,800
Pervaporation Unit						
Membrane Area (m^2)	16	30	60	60	75	95
Total Direct Cost ($)	5,183	9,718	19,435	19,435	24,294	30,772
Condenser						
Condenser Area (m^2)	16	28	46	46	65	70
Total Direct Cost ($)	93,300	94,700	97,200	97,400	99,700	99,900
Reboiler						
Reboiler Area (m^2)	7.0	9.3	19	23	30	33
Total Direct Cost ($)	120,600	127,900	150,300	161,000	180,200	180,200
Middle Vessel						
Volume (L)	901	920	912	916	901	901
Total Direct Cost ($)	138,200	138,300	138,200	138,200	138,200	138,200
Cycle Performance						
Cycle Time (min)	403	241	148	111	81	64
Ethyl Lac. Produced (kmol/cyc.)	3.16	3.17	3.15	3.14	3.10	3.07
Cost Summary						
Total Manufacturing ($1,000/yr)	751	832	912	1,020	1,130	1,240
Total Capital ($1,000)	1,300	1,450	1,510	1,590	1,740	1,790
Total Lifetime ($1,000)	3,560	3,940	4,250	4,600	5,140	5,500

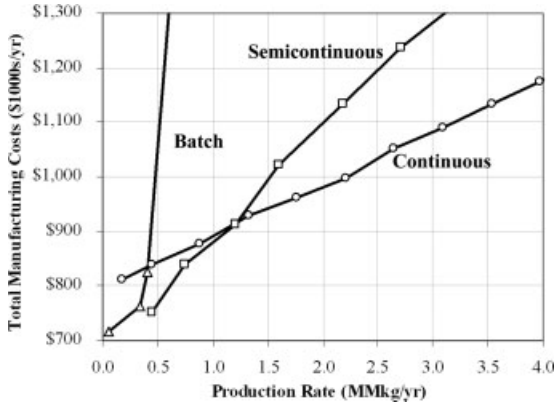

Figure 16. Annual manufacturing costs of the three design types at various production rates.

to use multiple smaller units in parallel than to use a single, large batch unit. This follows well-known heuristics and is the reason why continuous systems are typically used rather than batch processes at larger production rates. Considering a three year lifetime, the SD process has the lowest total lifetime cost for capacities between 0.3 and about 2.0 MM kg/yr, as shown in Figure 18.

Conclusions

The feasibility of using semicontinuous distillation to produce and isolate ethyl lactate has been demonstrated. Rigorous simulations and cost estimations suggest that this technique is economically preferable to traditional batch and continuous alternatives for a wide range of production rates. The key innovation lies in the use of a middle vessel interactively with a single distillation column to achieve a ternary separation. This technique can be further extended to any multi-species system where azeotropic boundaries are not crossed. Because of the potential for significant cost savings at intermediate capacities, SD should be considered for production of fine and specialty chemicals.

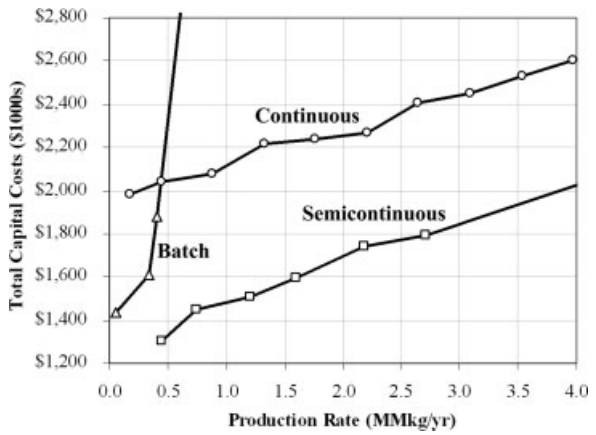

Figure 17. Total capital costs of the three design types at various production rates.

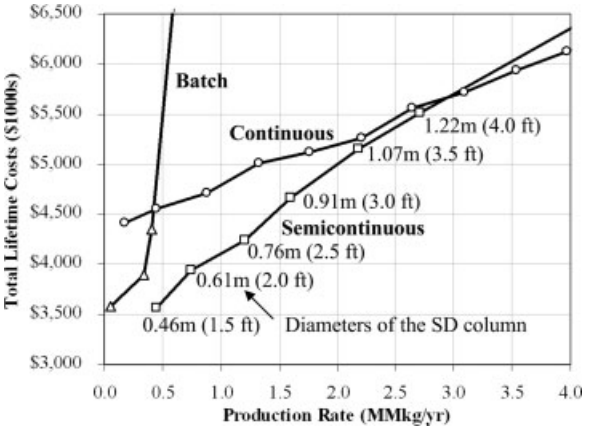

Figure 18. Total lifetime costs of the three design types at various production rates. The diameters at the bottom of the column for the SD cases are annotated.

Acknowledgments

This study was partially funded by a National Science Foundation Graduate Fellowship.

Notation

Abbreviations

CSTR = continuous stirred-tank reactor
E = ethanol
EL = ethyl lactate
LA = lactic acid
MV = middle vessel
PI = proportional-integral
PFR = plug-flow reactor
PSS = pseudo steady state
RD = reactive distillation
S = catalytically active site
SD = semicontinuous distillation
SDRMV = semicontinuous distillation with reaction in a middle vessel
VLE = vapor-liquid equilibria
W = water

Variables

a = constant in kinetic Eq. 5 (L/kmol)
A_m = membrane transfer surface area (m^2)
b = constant in permeance equations
c = constant in controller equations
C = molar concentration (kmol/L)
D = actual column diameter (m)
D_{min} = minimum column diameter necessary to prevent flooding (m)
e = error (difference from setpoint) in a measured variable ($x - x_{Sp}$)
E = activation energy (kJ/mol)
f = function
F = molar flow rate (kmol/min)
g_0 = coefficient in Eq. 7 (kJ/mol)
g_1 = coefficient in Eq. 7 [kJ/(mol K)]
ΔG° = Gibbs free energy of reaction in the standard state (kJ/mol)
ΔH_A = heat of adsorption, see Eq. 5 (kJ/mol)
$\underline{\underline{J}}$ = Jacobean matrix
k = rate constant (min^{-1})
k_0 = rate constant [L/(min kg)]

K = equilibrium constant
K_{A0} = pre-exponential factor for adsorption equilibrium constant, see Eq. 5 (L/kmol)
Kc = controller gain
m = mass flow rate (kg/min)
MW = molecular weight (g/mol)
N = number of chemical species
P = pressure (bar)
P^* = vapor pressure (bar)
$\overline{P}_i$ = permeance [kg/(m^2 min bar)]
r = intrinsic rate of reaction [kmol/(L min)]
R = ratio; universal gas constant
t = time (min)
T = temperature (K)
V = volume (L)
w = weight ratio (kg/kg); weight fraction
x = liquid mole fraction
y = vapor mole fraction
$\underline{z}$ = vector of unknowns in Newton–Raphson equations

Greek letters

γ = liquid-phase activity coefficient
δ_i^k = the Kroeneker delta function ($\delta_i^k = 0, i \neq k$; $\delta_i^k = 1, i = k$)
ρ = density (kg/L)
τ_I = controller integral time constant (min^{-1})

Subscripts

B = bottoms
boil = boilup
cat = catalyst
D = distillate
E = ethanol
EL = ethyl lactate
eq = equilibrium
F = feed
i, j, k = species counters (E, LA, W, or EL)
LA = lactic acid
liq = liquid
max = maximum allowed
P = permeate
pot = still pot
R = retentate
ref = reflux
S = side draw
Sp = setpoint
W = water

Literature Cited

1. Chang J. Specialties hitting sweet spot. *Chem Market Reporter*. 2005;267:25:10.
2. Van Savage E. Demand for gases rising in specialty markets and Asia. *Chem Market Reporter*. 2004;265:3:14.
3. Scott A. Fine and specialty chemical optimism rises. *Chem Week*. 2004;166:37.
4. Phimister JR, Seider WD. Semicontinuous, middle-vessel distillation of ternary mixtures. *AIChE J*. 2000;46:1508–1520.
5. Phimister JR, Seider WD. Distillate-bottoms control of middle-vessel distillation columns. *Ind Eng Chem Res*. 2000;39:1840–1849.
6. Phimister JR, Seider WD. Bridge the gap with semicontinuous distillation. *Chem Eng Prog*. 2001;97:72–78.
7. Monroy-Loperena R, Alvarez-Ramirez J. Some aspects of the operation of semi-continuous, middle-vessel distillation columns. *Chem Eng Commun*. 2004;191:1437–1455.
8. Phimister JR, Seider WD. Semicontinuous, middle-vessel, extractive distillation. *Comput Chem Eng*. 2000;24:879–885.
9. Phimister JR, Seider WD. Semicontinuous, pressure-swing distillation. *Ind Eng Chem Res*. 2000;39:122–130.
10. Adams TA, Seider WD. Semicontinuous distillation with chemical reaction in a middle vessel. *Ind Eng Chem Res*. 2006;45:5548–5560.
11. Tanaka K, Yoshikawa R, Ying C, Kita H, Okamoto K-I. Application of zeolite T membrane to vapor-permeation-aided esterification of lactic acid with ethanol. *Chem Eng Sci*. 2002;57:1577–1584.
12. Vu DT, Lira CT, Asthana NS, Kolah AK, Miller DJ. Vapor-liquid equilibria in the systems ethyl lactate + ethanol and ethyl lactate + water. *J Chem Eng Data*. 2006;51:1220–1225.
13. Keyes DB. Esterification processes and equipment. *Ind Eng Chem*. 1932;24:1096–1103.
14. Benedict DJ, Parulekar SJ, Tsai S-P. Esterification of lactic acid and ethanol with/without pervaporation. *Ind Eng Chem Res*. 2003;42:2282–2291.
15. Jafar JJ, Budda PM, Hughes R. Enhancement of esterification reaction yield using zeolite A vapour permeation membrane. *J Membr Sci*. 2002;199:117–123.
16. Sanchez-Daza O, Escobar GV, Zarate EM, Munoz EO. Reactive residue curve maps, a new study case. *Chem Eng J*. 2006;117:123–129.
17. Gao J, Zhao XM, Zhou LY, Huang ZH. Investigation of ethyl lactate reactive distillation process. *Chem Eng Res Des*. 2007;85:525–529.
18. Adams TA. Animation of ethyl lactate semicontinuous distillation case study for 4 ft. column. http://www3.interscience.wiley.com/journal/120848573/suppinfo. 2007.
19. Wankat PC. *Equilibrium Staged Separations: Separations in Chemical Engineering*. New York: Elsevier, 1988:707.
20. Peña-Tejedor S, Murga R, Sanz MT, Beltrán S. Vapor-liquid equilibria and excess volumes of the binary systems ethanol + ethyl lactate, isopropanol + isopropyl lactate and *n*-butanol + *n*-butyl lactate at 101.325 kPa. *Fluid Phase Equil*. 2005;230:197–203.
21. Bausa J, Marquardt W. Detailed modeling of stationary and transient mass transfer across pervaporation membranes. *AIChE J*. 2001;47:1318–1332.
22. Takaba H, Koyama A, Nakao S-I. Dual ensemble Monte-Carlo simulation of pervaporation of an ethanol/water binary mixture in silicalite membrane based on a Lennard-Jones interaction model. *J Phys Chem B*. 2000;104:6353–6359.
23. Nakrachi A, Hus P, Belkoura L, Souchon I, Voilley A. Modelling and simulation of a membrane separation process. Case study; the pervaporation. In: *Proceedings of 12th International Conference on Systematic Science*, Wroclaw, Poland, 1995;433–439.
24. Wijmans JG, Baker RW. Simple predictive treatment of the permeation process in pervaporation. *J Membr Sci*. 1993;79:101–113.
25. Guan H-M, Chung T-S, Huang Z, Chng ML, Kulprathipanja S. Poly (vinyl alcohol) multilayer mixed matrix membranes for the dehydration of ethanol-water mixture. *J Membr Sci*. 2006;268:113–122.
26. Levenspiel O. *Chemical Reaction Engineering*, 3rd ed. New York: Wiley, 1999.
27. Adams TA. Animation of ethyl lactate semicontinuous distillation column profile for 4 ft. column. http://www3.interscience.wiley.com/journal/120848573/suppinfo. 2007.
28. GFS Chemicals Product Catalogue: Amberlyst 15 Ion Exchange Resin #2652. http://www.gfschemicals.com/chemicals/gfschem-2652.asp. Accessed July 2005.
29. Seider WD, Seader JD, Lewin DR. *Product and Process Design Principles: Synthesis, Analysis, and Evaluation, 2nd ed*. New York: Wiley, 2004.

Manuscript received July 2, 2007, and revision received May 7, 2008.